

Figure S1. HAS2 is upregulated in response to CD44s overexpression. (A) Table showing the top 10 upregulated genes in response to CD44s overexpression in Mes10A cells. Fold change is relative to control Mes10A cells. (B) HAS2 expression remained similar in CD44v-overexpressing cells to that in control cells. Error bars indicate SD; n=3.

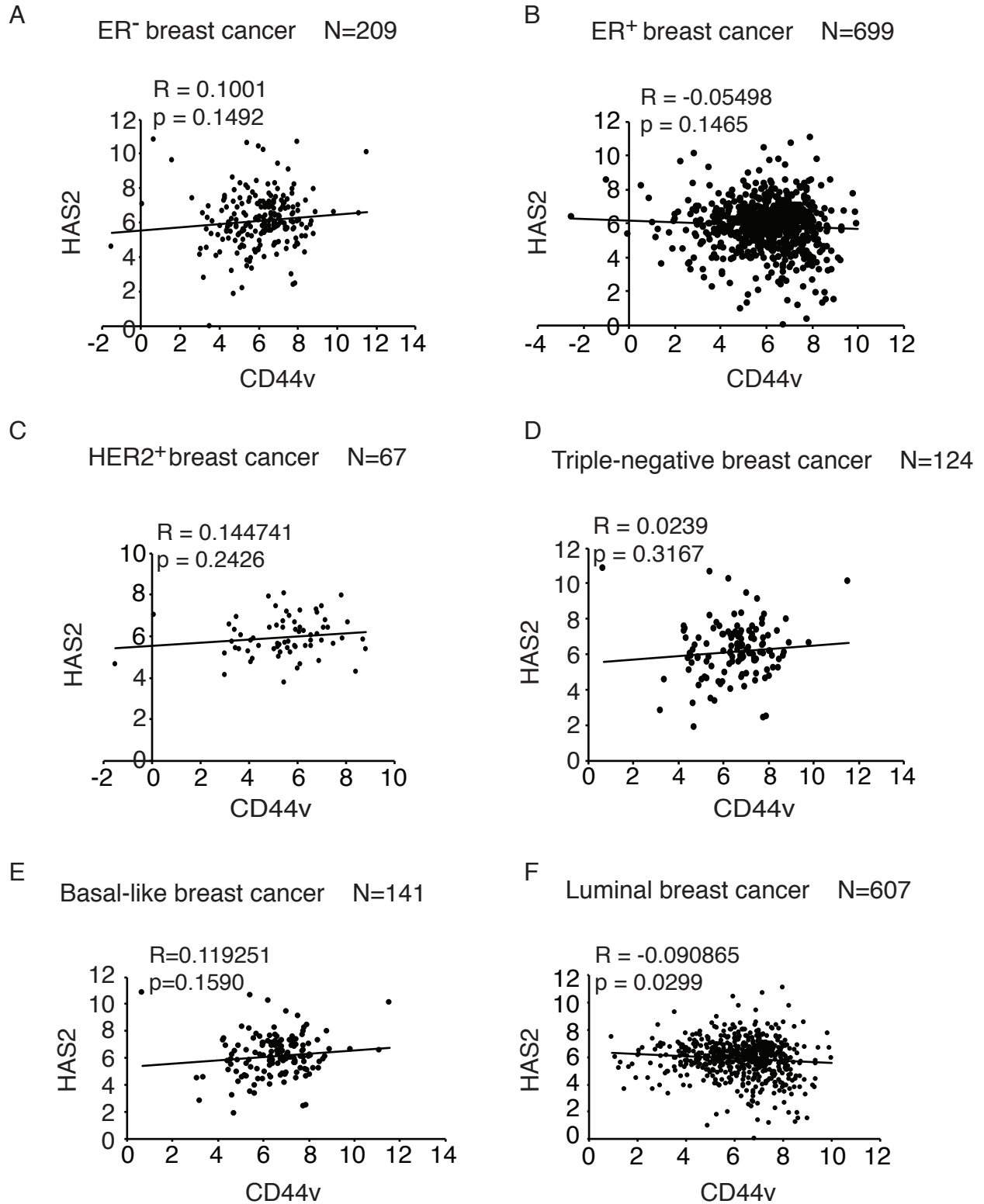


Figure S2. TCGA data analysis of CD44v and HAS2 expression in breast cancer. Data show that CD44v and HAS2 are not correlated in ER⁻ (A), ER⁺ (B), Her2⁺ (C), Triple-negative (D), Basal-like (E), or Luminal (F) breast cancer subtypes.

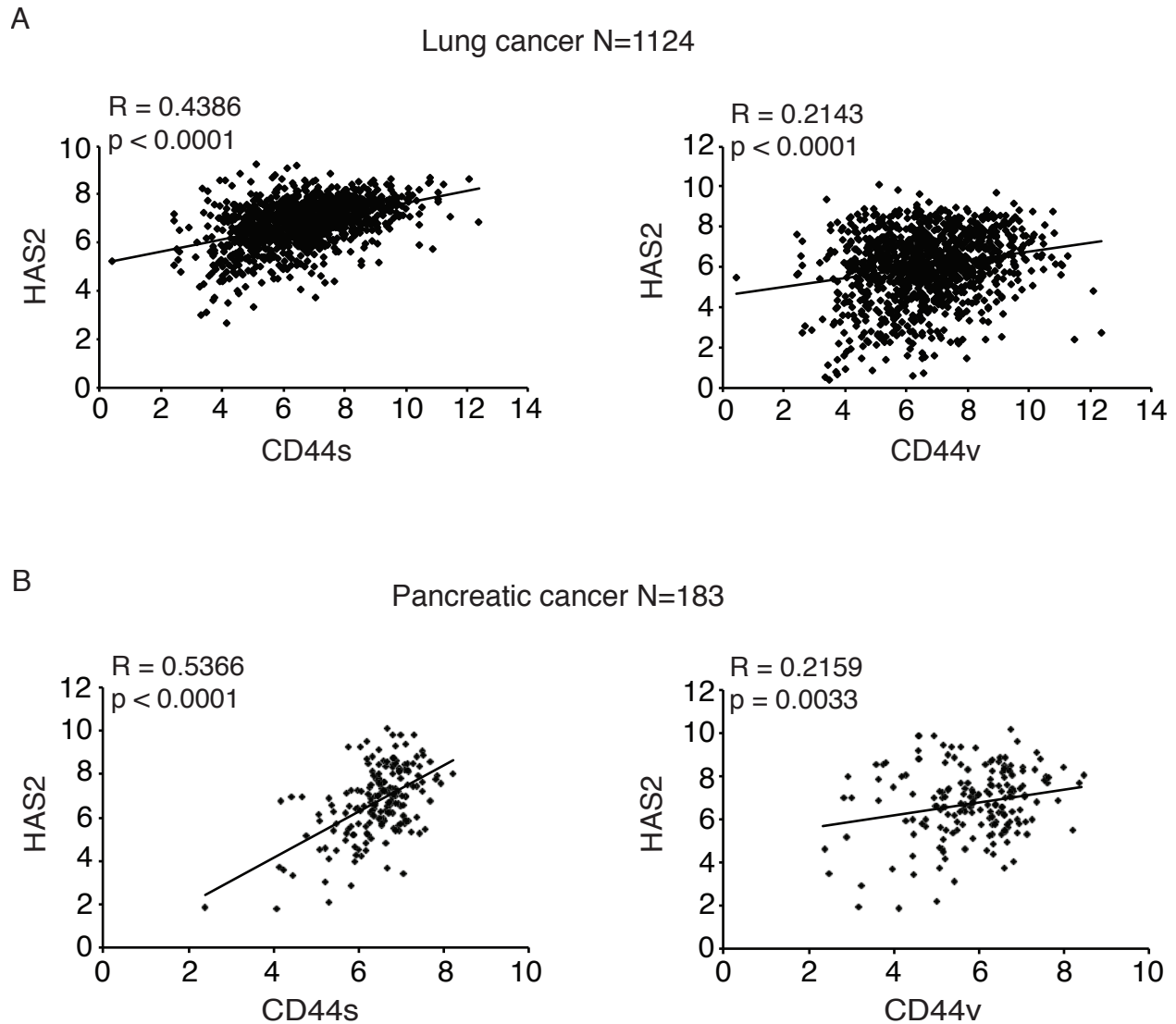


Figure S3. TCGA data analysis of CD44 isoforms and HAS2 expression. Data show that HAS2 expression is more positively correlated with CD44s than that with CD44v in lung cancer (A) and pancreatic cancer (B).

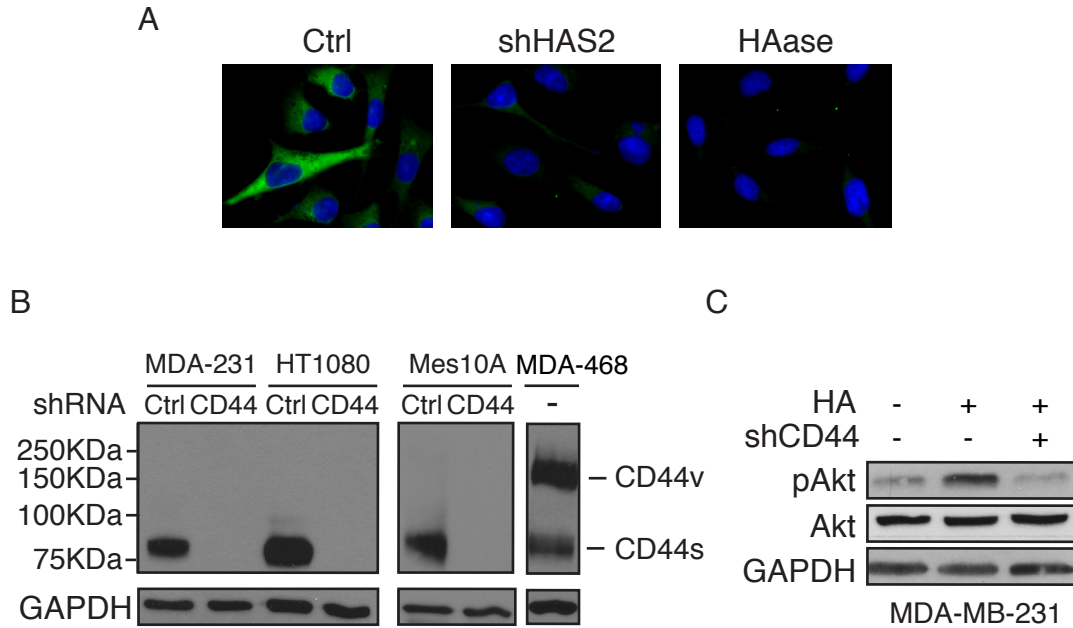


Figure S4. HAS2/HA activates Akt signaling in a CD44s-dependent manner. (A) Immunofluorescent images showing levels of HA in control, HAS2 shRNA-expressing, and HAase-treated (100 μ g/ml, 6 h) LM2 cells. HA was visualized by AF488-HABP (green). DAPI staining (blue) indicates nuclei. (B) Immunoblot analysis showing that CD44s is detected in MDA-MB-231, HT1080, and Mes10A cells, and that CD44 shRNA effectively knocked down CD44s. As a reference, an immunoblot of CD44s and CD44v, which are both expressed in MDA-MB-468, is shown on the right. (C) Immunoblot analysis of Akt activation in M DA-MB-231 cells that were plated on HA-coated plates (0.1 mg/ml HA). 24 h after plating, cells were stimulated with insulin stimulation (10 μ g/ml) for Akt activation.

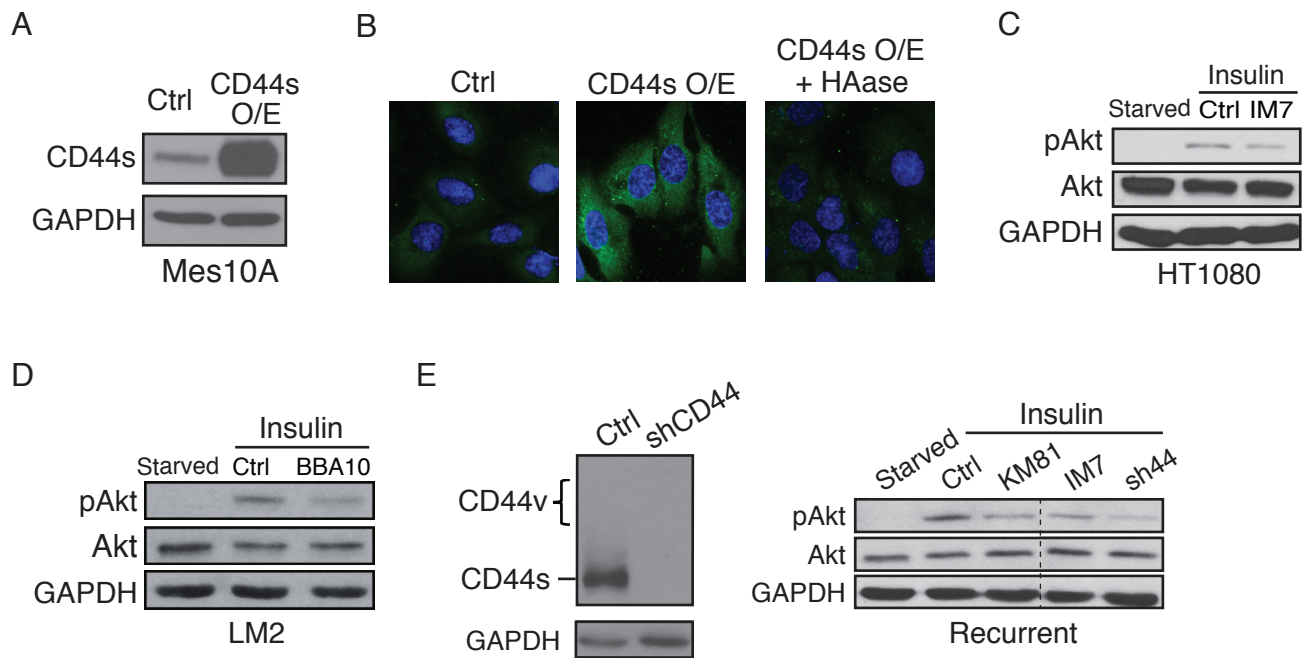


Figure S5. CD44s-mediated Akt activation is attenuated by depletion of HA or addition of CD44 antibodies. (A) Immunoblot analysis showing CD44s levels in control and CD44s overexpression Mes10A cells. (B) Immunofluorescent images showing levels of HA in control, CD44s-overexpressing, and HAase-treated CD44s-overexpressing Mes10A cells. HA was visualized by AF488-HABP (green). DAPI staining (blue) indicates nuclei. (C) Immunoblot analysis of Akt activation in HT1080 cells that were starved overnight, treated with the IM7 anti-CD44 antibody (10 $\mu\text{g/ml}$, 3 h), and stimulated with insulin (10 $\mu\text{g/ml}$, 30 min). (D) Immunoblot analysis of Akt activation in LM2 cells that were starved overnight, treated with the BBA10 anti-CD44 blocking antibody (5 $\mu\text{g/ml}$, 3 h), and stimulated with insulin (10 $\mu\text{g/ml}$, 30 min). (E) *Left panel:* Immunoblot images showing CD44s depletion in CD44 shRNA-expressing recurrent tumor cells. *Right panel:* Recurrent cells were starved overnight, subjected to antibody treatment (KM81: 1 $\mu\text{g/ml}$ and IM7: 10 $\mu\text{g/ml}$, 3 h), and stimulated with insulin (10 $\mu\text{g/ml}$, 30 min). CD44 knockdown cells were used as a positive

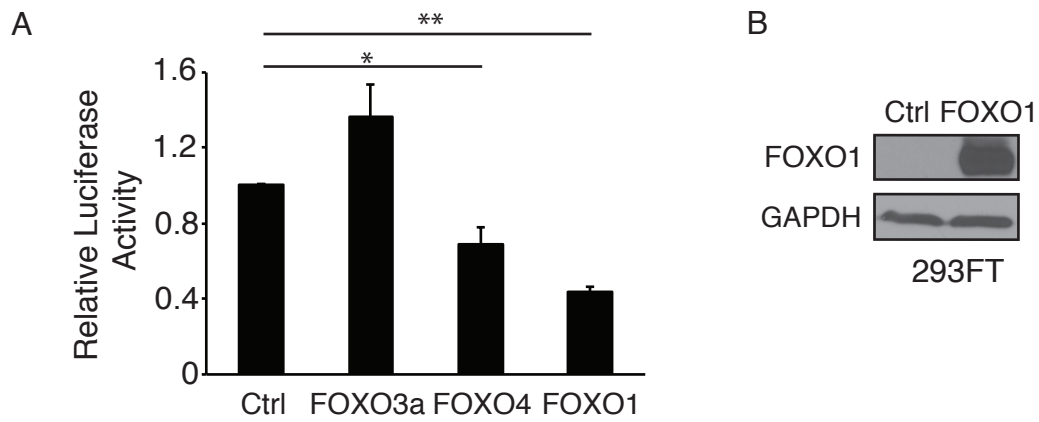


Figure S6. Effects of FOXO family proteins on HAS2 promoter activity. (A) Relative luciferase activity were shown in 293FT cells that were transfected with a HAS2 luciferase reporter construct and transcription factors FOXO3a, FOXO4 and FOXO1. Error bars indicate SD; n=3. (B) Immunoblot analysis showing levels of FOXO1 overexpression in 293FT cells that were used for ChIP analysis.

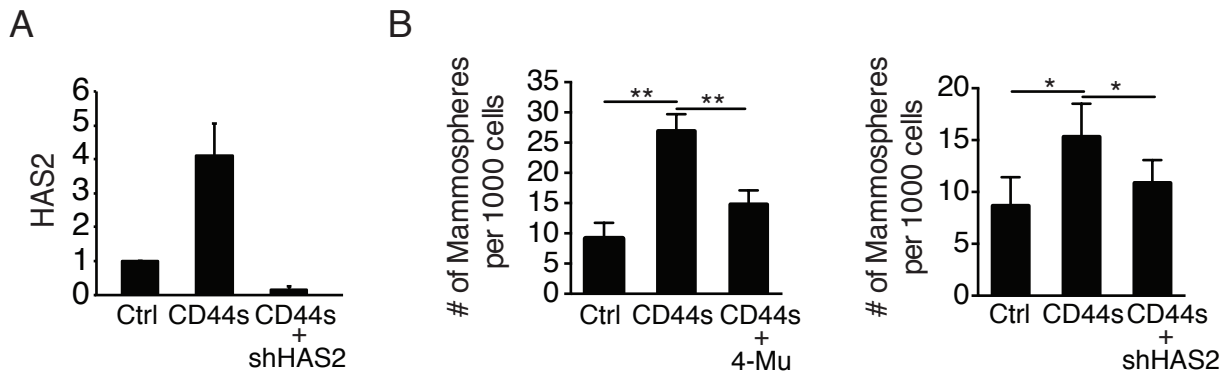


Figure S7. Inhibition of HAS2 reduces mammosphere forming ability. (A) qRT-PCR analysis of HAS2 expression in CD44s-overexpressing Mes10A cells that expressed HAS2 shRNA. Error bars indicate SD; n = 3. (B) Mammosphere formation assay showing that addition of the HAS2 inhibitor 4-Mu (0.4 mM, left panel) or depleting HAS2 by shRNA (right panel) abolished the effect of CD44s on promoting mammosphere formation. Data are average of three independent experiments. All error bars indicate SEM; n=3. *p < 0.05, **p < 0.01.